

The distribution of impurities in the interfaces and window layers of thin-film solar cells

M. Emziane,^{a)} K. Durose, and D. P. Halliday

Department of Physics, University of Durham, South Road, Durham, DH1 3LE, United Kingdom

N. Romeo and A. Bosio

INFN, Department of Physics, University of Parma, Parco Area delle Scienze 7a, 43100 Parma, Italy

(Received 26 October 2004; accepted 25 March 2005; published online 1 June 2005)

We report a systematic multielement study of impurities in CdS window layers by dynamic and quantitative secondary-ion-mass spectrometry (SIMS) with high depth resolution. The study was carried out on CdTe/CdS solar cell structures, with the glass substrate removed. The analysis proceeded from the transparent conductive oxide free surface to the CdTe absorbing layer with a view to examining the influence of the CdCl₂ heat treatment on the distribution and concentration of impurities in the structures. Special attention was paid to the impurities present in the CdS window layer that may be electrically active, and therefore affect the characteristics of the CdTe/CdS device. It was shown that Cl, Na, and Sb impurities had higher concentrations in CdS following cadmium chloride (CdCl₂) heat treatment while Pb, O, Sn, and Cu conserved the same concentration. Furthermore, Zn, Si, and In showed slightly lower concentrations on CdCl₂ treatment. Possible explanations of these changes are discussed and the results compared with previous SIMS measurements from the “back wall” (i.e., from the CdTe free surface through the glass substrate) obtained from the same structures. © 2005 American Institute of Physics. [DOI: 10.1063/1.1921344]

I. INTRODUCTION

The conventional processing of semiconductors relies on the ability to control impurities which are usually present in the devices at higher concentrations than are in the starting materials. The use of polycrystalline thin films for solar cells aims to reduce the cost by utilizing lower grade source materials. The irreproducibility of the characteristics of such devices and their degradation have yet to be addressed.

Postgrowth annealing-induced activation of thin-film CdTe/CdS solar cells with CdCl₂ represents a crucial step in the device fabrication process. This treatment has been shown to affect not only the CdTe absorbing layer but also the CdS window layer, leading to a change in the cell characteristics.¹ It is the impurities in the window layer that are the subject of this paper.

The effect of impurities present in the CdS window layer on CdTe-based solar cell devices has not been thoroughly investigated, and it is not yet fully understood in terms of their influence on the efficiency, stability, and lifetime of these devices.² Nevertheless, some particular studies point to the importance of impurities in this context. For example, the photovoltaic characteristics of CdTe/CdS solar cells fabricated using boron-doped CdS were shown to improve due to the increase of the electrical conductivity and the optical band gap of the CdS with doping.³ Also, some test cells composed of *p*-type Cu-doped CdS and *n*-type CdS layers were fabricated and their photovoltaic response attributed to a homojunction.⁴ Indirect effects have also been noted: for example, CdS surface contamination and chemical composi-

tion were shown to depend on the growth method used.⁵ Additionally, the surface morphology and pretreatment of the transparent conductive oxide (TCO) have been found to affect the physical properties of the CdS film subsequently deposited on it, eventually changing the performance of CdTe/CdS solar cells.⁶

Despite the importance of impurities in semiconductors, few attempts to measure them in CdTe/CdS devices have been reported in the literature. In particular, there is little systematic or quantitative work, with secondary-ion-mass spectroscopy (SIMS), profiles on entire device structures being generally restricted to a few impurity elements and done through the “back wall,” i.e., proceeding from the CdTe surface. This back wall approach has limitations—principally a poor depth resolution due to the roughness of the back surface and the large depth that has to be profiled to get to the buried CdTe/CdS interface. To overcome this difficulty, polished CdTe surfaces were used,⁷ but only one SIMS analysis from the “front wall,” i.e., by sputtering from the TCO to the semiconductors, has been reported.⁸

This paper reports a systematic quantitative study of impurities in the window layers of CdTe/CdS/TCO/glass solar cells, this also being done with sufficient depth resolution to identify interface effects. This was achieved by dynamic and quantitative SIMS of CdTe/CdS/TCO/glass structures in the front wall geometry after the removal of the glass substrate. The analysis was then performed from the (flat) TCO free surface through the CdTe absorbing layer. Particular emphasis was placed on the potentially electrically active impurities present in the CdS window layer especially those likely to originate from the CdCl₂ heat treatment; it is these impurities that are likely to affect the device performance.

^{a)}Electronic mail: m.emziane@dur.ac.uk

In this way the distributions and concentrations of a number of impurities in the window layer of CdTe/CdS/TCO/glass cells were determined with higher precision than before.

It was found that Cl, Na, and Sb impurities had higher concentrations in CdS following CdCl₂ heat treatment while Pb, O, and Cu conserved the same concentration. While Na and Si were apparently concentrated at the CdS interfaces in the as-grown structures, they had a concentration peak in the CdS after treatment. Also, Zn, Si, and In showed slightly reduced concentrations on the CdCl₂ heat treatment. Te diffusion into the CdS layer on the CdCl₂ heat treatment was also measured.

The potential origins of these impurities and their concentration changes are discussed. For instance, it was shown that Si and Na were originating mainly from the glass substrate during the growth and/or processing steps, and that In and O were due mostly to the TCO. A useful comparison was made between the present results and the SIMS measurements previously obtained on similar structures from the back wall.⁹ Moreover, the displacement of the positive- and negative-ion concentration peaks reported earlier¹⁰ and the accumulation of Sb at the CdS/TCO interface¹¹ are called into question.

II. EXPERIMENT

The TCO (In₂O₃:F, nominally 800 nm thick) and CdS (nominally 150 nm thick) layers were grown by sputtering with a typical substrate temperature of 500 and 200 °C, respectively. The target purity was 99.999% for In₂O₃ and 99.99% for CdS. We used two uncontacted CdTe/CdS/TCO/glass solar cell-like structures fabricated separately using nominally identical conditions. The deposition and processing conditions were the same as reported earlier in more detail.⁹ Polycrystalline CdTe films were deposited on the CdS/TCO/glass substrates by close-space sublimation (CCS) technique. The substrate and source temperatures during the deposition were kept at 500 and 650 °C, respectively. The deposition rate was adjusted at about 2 μm/min and the thickness of the CdTe films was approximately 8–10 μm. Both structures had their CdTe layer deposited using a starting CdTe material of 7N purity (i.e., 99.999 99%) and one of them only was then heat treated with CdCl₂ (thermally evaporated 150-nm-thick CdCl₂ layer, 99.9% pure) at 400 °C in air for 30 min, and subsequently chemically etched with Br₂-methanol solution. This was carried out in order to study the effect of the CdCl₂ and chemical etching process on the impurity distribution in the whole solar cell structure. To enable a SIMS investigation of both samples from the front wall side, i.e., from the TCO layer through the CdS and CdTe layers, the glass substrates were removed by a combined mechanical and chemical polishing procedure. To do so, the CdTe surfaces of the 1-cm² samples were stuck to aluminum plates using conductive epoxy to avoid charging during the SIMS measurements. Most of the glass was removed by mechanical polishing and during the removal of the remainder with 40% HF acid, the TCO layer acts as an etch-stop barrier.

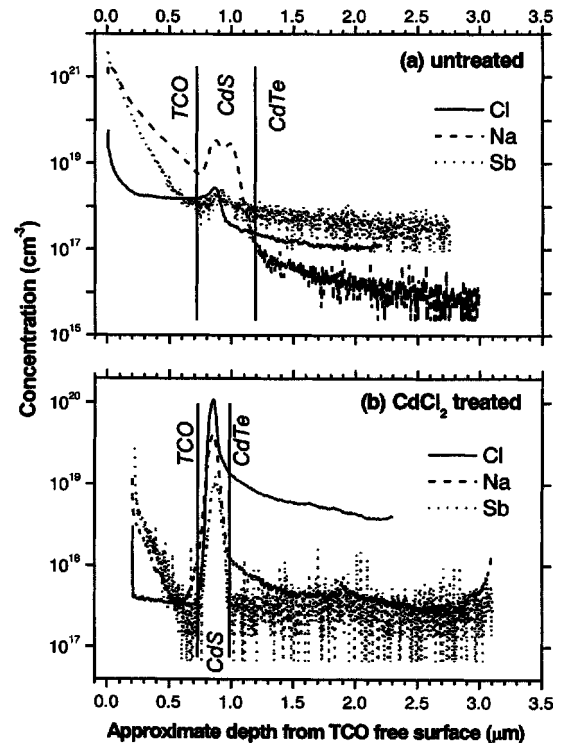


FIG. 1. Impurity species showing an increased concentration following the CdCl₂ heat treatment. The SIMS depth profiles of Cl, Na, and Sb impurity atoms for the CdTe/CdS/TCO structures untreated (a) and CdCl₂ heat treated (b). The TCO free surface is nearest the zero end, and the approximate locations of the interfaces are shown by the vertical solid lines. The profiles of the treated structure were shifted forward to align with those of the untreated sample at the CdS/TCO interface.

The SIMS depth profiles were performed using a Cameca ims-4f system on both the untreated and CdCl₂ heat-treated CdTe/CdS/TCO structures. Profiles of ²⁰⁸Pb, ¹²⁸Te, ¹²¹Sb, ¹¹⁸Sn, ¹¹⁵In, ⁶⁶Zn, ⁶³Cu, ³⁷Cl, ³⁴S, ²⁸Si, ²³Na, and ¹⁸O were recorded. Ion-implanted undoped CdS standards were depth profiled to determine the “useful ion yields” of the elements and were used to perform quantitative interpretation of the raw data recorded through the use of relative sensitivity factors (RSFs). Implantations were performed at room temperature using a 200-keV implanter and low doses were used to obtain a maximum concentration level of 10¹⁸ cm⁻³ for all the species considered. An oxygen primary beam was used to determine the positive-ion yield and a cesium primary beam for the negative ions. Energies and analyzed crater areas were as follows: 14.5 keV and ~60 × 60 μm² for Cs⁺, and 8 keV and ~150 × 150 μm² for O²⁺.

III. RESULTS

During the SIMS profiling it became clear that although the layers were nominally identical, the thicknesses of both the TCO and CdS layers were thinner in the processed sample than in the as-grown one. For ease of comparison, the SIMS data presented in Figs. 1–4 are therefore shifted so that pairs of profiles are aligned at the CdS/TCO interface. Moreover, it should be noted that for some SIMS runs presented here, the complete structure was profiled, i.e., from the TCO all the way through the back wall of the CdTe. These profiles

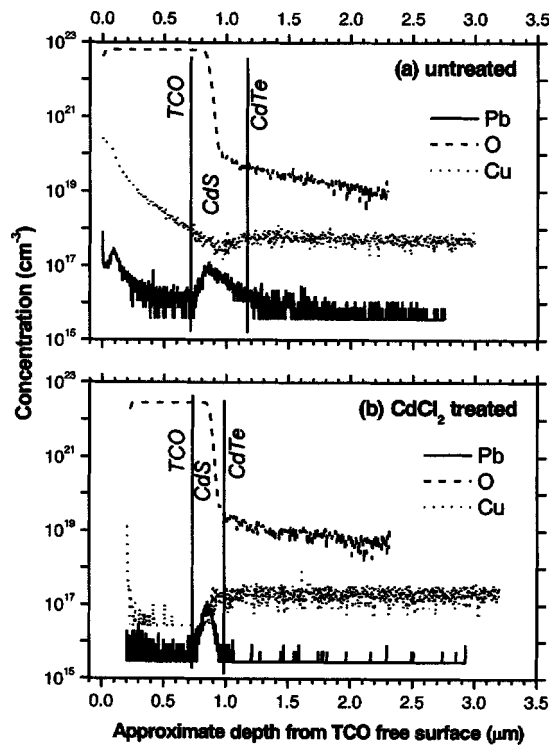


FIG. 2. Impurity species which have an unchanged concentration after CdCl_2 heat treatment. The SIMS depth profiles of Pb, O, and Cu impurity atoms for the CdTe/CdS/TCO structures untreated (a) and CdCl_2 heat treated (b). The profiles of the treated structure were shifted forward to match those of the untreated sample at the CdS/TCO interface. The TCO free surface is taken as depth zero and the approximate locations of the interfaces are shown by the vertical solid lines.

may be recognized since the apparent concentrations of the elements profiled rise slightly as the back wall of the CdTe is approached [e.g., as for Na in Fig. 1(b)].

The SIMS depth profiles of Na, Sb, and Cl atoms in the untreated (i.e., as-grown) and CdCl_2 heat-treated CdTe/CdS/TCO structures are shown in Fig. 1. These three species exhibit an increased concentration in the treated sample as compared to the untreated one. In the CdS layer, the concentration increases from 2.8×10^{18} to 10^{20} cm^{-3} for Cl and from 2×10^{18} to 10^{19} cm^{-3} for Sb. Na shows a very slight increase, from 3×10^{19} to $4 \times 10^{19} \text{ cm}^{-3}$. Similar results were obtained when the same elements were investigated from the CdTe free surface through the glass substrate⁹ (i.e., from the back wall of the structures). However, additional precision is obtained in the front wall geometry—the structure of the Na profile is discussed in Sec. IV.

Figure 2 displays the SIMS depth profiles of Pb, O, and Cu atoms in the untreated and CdCl_2 heat-treated CdTe/CdS/TCO structures. These three species have their concentration profile largely unchanged following the CdCl_2 heat treatment. The concentrations are 10^{17} and $3 \times 10^{17} \text{ cm}^{-3}$ for Pb and Cu, respectively. For O, the concentration decreases from $(3\text{--}6) \times 10^{22} \text{ cm}^{-3}$ near the CdS/TCO interface to $(3\text{--}6) \times 10^{19} \text{ cm}^{-3}$ near the CdTe/CdS interface, the trend being the same before and after the heat treatment. Profiles of Sn are not shown because they overlap each other, do not show any peaks, and are noisy around 10^{17} cm^{-3} , below the Sn detection limit. In our previous SIMS study from the back

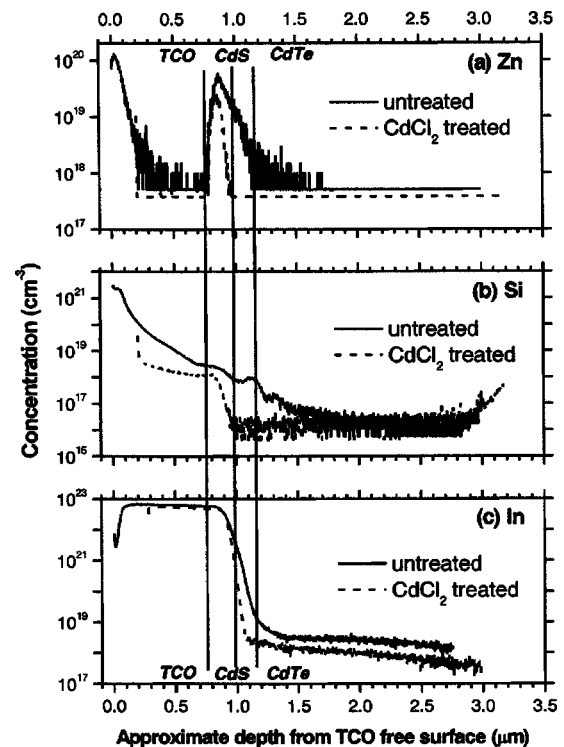


FIG. 3. Impurity species showing a reduced concentration after the CdCl_2 heat treatment. The SIMS depth profiles of Zn, Si, and In impurity atoms for the untreated and CdCl_2 heat treated CdTe/CdS/TCO structures. The profiles of the treated structure were shifted to match those of the untreated sample at the CdS/TCO interface. Since the CdS layer is thinner in the treated structure compared to the untreated one, an additional vertical line shows the approximate CdTe/CdS interface for the treated structure.

wall,⁹ these four impurity elements showed a constant concentration in CdTe on the CdCl_2 heat treatment.

The SIMS depth profiles of Zn, Si, and In atoms are shown in Fig. 3 for both the untreated and CdCl_2 heat-treated CdTe/CdS/TCO structures. Surprisingly, Zn, Si, and In show apparent small decreases in concentration in CdS upon the CdCl_2 heat treatment in comparison to the untreated samples. Within CdS, the concentrations are $(2\text{--}5) \times 10^{19} \text{ cm}^{-3}$ for Zn, $(1\text{--}2) \times 10^{18} \text{ cm}^{-3}$ for Si, and $10^{19}\text{--}10^{22} \text{ cm}^{-3}$ for In. The detection of Zn and Cu in CdTe and the TCO was limited by the detection limit in these layers, with the profiles being characteristically noisy and flat.

The SIMS profiles for Te and S atoms in both CdTe/CdS/TCO structures are shown in Fig. 4. The different layers and approximate interfaces are shown in all the figures. The depth scale is accurate from the TCO free surface to the CdS/TCO interface as the sputtering rate of TCO was used to generate the depth scale. Since the TCO sputtering rate is different from the CdS and CdTe rates, the total depth sputtered in the CdS and CdTe layers is therefore different from that shown in all the figures.

Overall, the front wall SIMS profiles shown in the figures exhibit less surface tailing compared to the profiles recorded for two similar structures from the CdTe back surface and reported earlier.⁹ An additional advantage is that the positions and widths of the buried CdS/TCO and CdTe/CdS interfaces, together with the approximate thickness of the different layers, are more accurately determined here in com-

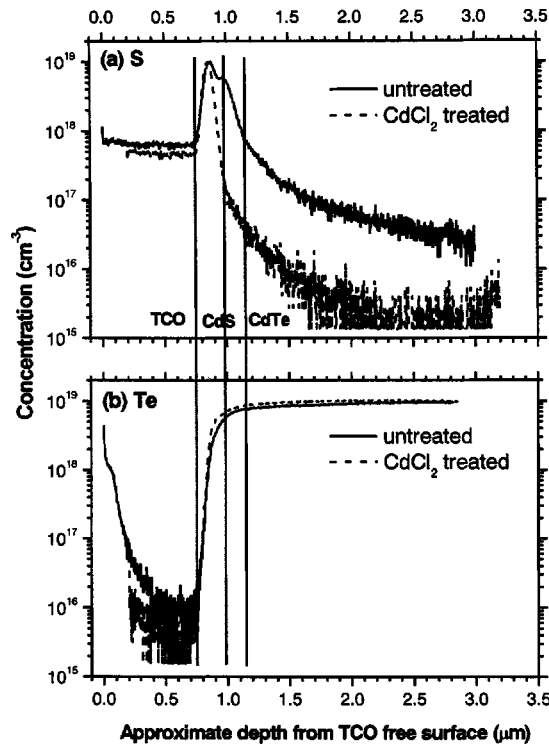


FIG. 4. Te diffusion at the CdTe/CdS interface. The SIMS depth profiles of Te and S atoms for the CdTe/CdS/TCO structures untreated and CdCl₂ heat treated. The profiles of the treated structure were shifted to align with the profiles of the untreated sample at the CdS/TCO interface, and an additional vertical line shows the approximate CdTe/CdS interface for the treated structure. Note also that S concentration in CdS is in a. u. instead of cm⁻³.

parison with those extracted from the back wall SIMS.⁹ This can be attributed to SIMS profiling commencing from the flat TCO free surfaces that are exposed by the glass removal process, while in our previous study, the CdTe surfaces (i.e., starting point for SIMS measurements from back wall) were rough and were not polished.⁹ Moreover, sputtering in the front wall geometry, i.e., through ~950 nm of TCO and CdS, is not subject to the crater roughening that inevitably happens during sputtering through 8–10 μm of CdTe.⁹ Hence front wall SIMS provides superior spatial definition of impurities in the CdS window layer and its interfaces than does back wall SIMS.

In a recent study using inductively coupled plasma mass spectrometry (ICPMS),¹² we have carried out a chemical analysis of the CdCl₂ powder used in this study. For the impurity species considered in the present investigation, the concentrations recorded in the CdCl₂ are summarized in Table I. Note that In and Te concentrations represent the maximum values, i.e., the actual ones may well be lower due to the possible spectral interferences occurring in ICPMS as previously discussed in detail.¹²

IV. DISCUSSION

In discussing the SIMS results, it should be emphasized that for all the profiles shown in the present study, the analysis is *quantitative* for the CdS layers only and *qualitative* for the other layers, i.e., TCO and CdTe, as only RSFs for CdS

TABLE I. Concentrations, in ppm units, of impurity species detected by ICPMS in the CdCl₂ powder used in the heat treatment of one of the samples.

Impurity species	Concentration (ppm)
Pb	116.59
Na	5.26
Te	2.51
In	0.94
Cu	0.28
Sb	0.21
Si, Sn, O, S, and Zn	Not detected

were used for the quantification of the SIMS data throughout the structures.

The purpose of this study was to focus on the impurities that have a known effect on the electrical (and most probably on the optical) properties of the CdS window layer and that may therefore affect the CdTe/CdS device characteristics. By using CdTe source material of 7N purity to grow CdTe/CdS/TCO/glass structures and treating part of them with CdCl₂, we were able to distinguish not only the impurities that are related to the CdCl₂ process, but also those due to the different layers in the structure.

Na, Sb, and Cl impurities shown in Fig. 1 might be considered to originate from the postgrowth processing as they are present in the CdCl₂ powder used. However, as shown in Table I, Na and Sb are present in the CdCl₂ powder with concentrations of 5.26 and 0.21 ppm, i.e., about 10¹⁷ and 5 × 10¹⁵ cm⁻³, respectively. These concentrations are more than two to three orders of magnitude lower in the CdCl₂ starting powder compared to those for the same elements measured in the CdS matrix by SIMS (Fig. 1). It is clearly the case that if Na and Sb arise solely from the CdCl₂ then either (a) these elements are enriched in the CdS during the treatment, perhaps by preferential evaporation onto the cells when they are coated with CdCl₂ before heating, or (b) these elements are not uniformly distributed throughout the CdTe/CdS layer stack, and that there is some preferred segregation at the CdS layer and/or its interfaces. One or both of (a) and (b) are credible in that the concentration of Na, and most notably of Sb, increase during the treatment. However, as the levels of both of these elements are already high in the as-grown structures, they may well have multiple origins. For Na, the glass is the most obvious source, with incorporation of glass components in the CdS being a possibility during the growth of the TCO and CdTe layers at a relatively high temperature. For Sb, a contamination from the CdS target during the sputter deposition of CdS layer is more likely as the target used is 99.99% pure.

The present findings for Pb, O, Cu, and Sn in CdS are consistent with those measured for CdTe from the back wall (i.e., invariant concentration profile on CdCl₂ heat treatment),⁹ and these four impurity elements are therefore not considered due to the CdCl₂ heat treatment as they conserve the same concentration for both samples.

It is interesting to compare the impurity concentrations we recorded by SIMS with some data available in the literature. The only quantitative SIMS analysis performed on

CdTe/CdS solar cell devices from the TCO side with the glass substrate removed was mainly dedicated to the determination of Cu profile.⁸ The Cu concentrations recorded in CdS were ranging from 2×10^{18} to 5×10^{19} cm⁻³, i.e., about one to two orders of magnitude higher than the Cu concentrations we measured in CdS (3×10^{17} cm⁻³, Fig. 2). The higher Cu concentrations in those structures were caused by the Cu diffusion from the Cu-containing back contact while our solar cell-like structures were uncontacted and contained no intentional Cu.

N, C, and O were also profiled in another quantitative SIMS analysis on CdTe/CdS solar cell devices fabricated using wet chemical methods.¹³ O concentrations were found to be in the range of 10^{20} – 10^{21} cm⁻³ throughout all the structures investigated, which is slightly higher than the O concentrations we obtained. This is because, in that study, the CdS layers were bath deposited (thus readily O contaminated) and air annealed prior to the CdTe growth. In our case, CdS was sputtered and was not air processed before the subsequent CdTe deposition by CSS. More importantly, that investigation concluded that there was neither an obvious correlation between the SIMS data and the device characteristics nor a simple relationship between the reagent concentrations in the CdS bath and the solar cell efficiency.¹³ For our structures, the O concentration in CdS ranged from $\sim(3\text{--}6) \times 10^{22}$ to $\sim(3\text{--}6) \times 10^{19}$ cm⁻³ while only 4×10^{18} cm⁻³ was measured in CdTe from the back wall.⁹ This indicates that O found in CdS may be coming from the In₂O₃:F TCO although incorporation from the growth (sputtering and CSS) and/or processing environments should not be excluded.

It was suggested that the *thickness* of the CdS window layer influences the formation of the CdTe_{1-x}S_x layer at the CdTe/CdS interface, as well as the CdTe grain growth (i.e., grain size and orientation), affecting the photovoltaic performance of the CdTe/CdS solar cell.¹⁴ Therefore, in discussing Zn, Si, and In concentrations in the untreated and CdCl₂ heat-treated structures shown in Fig. 3, it would be appropriate to take into account the difference in thickness for *both* TCO and CdS layers in the two structures. As mentioned above, these two layers are much thinner in the treated sample compared to the untreated one, and this may affect the comparison in terms of concentrations for these three impurity species. In order to check this behavior, normalized profiles (not shown here) were plotted for Zn, Si, and In assuming the same thickness for the CdS layer in both structures. This normalization confirmed the slight decrease of the concentration of the three elements following treatment. The SIMS data from the back wall showed that Zn conserved its concentration in the CdTe layer on the CdCl₂ heat treatment while Si and In concentrations increased following treatment. During the CdCl₂ treatment done at 400 °C, compounds such as ZnCl₂, InCl₃, and SiCl₄ may form, and while SiCl₄ is gaseous at this temperature, ZnCl₂ and InCl₃ have higher vapor pressure compared to CdCl₂. This is the most likely explanation of the decrease recorded in the concentration of Zn, Si, and In (Fig. 3) after the CdCl₂ treatment. Si [$(1\text{--}2) \times 10^{18}$ cm⁻³, Fig. 3] was not detected in the CdCl₂ powder (Table I) and its concentration is much higher than in

the CdTe layer as measured from the back wall (3×10^{15} – 4×10^{16} cm⁻³, below the detection limit),⁹ corroborating our previous interpretation that Si is mostly diffusing from the soda-lime glass substrate during the growth and/or the treatment of the structures, or else being transferred into the layers during sputter growth. As discussed above for Na, the diffusion of Si from glass is likely to take place since while the heat treatment is done at 400 °C for 30 min, the growth of the TCO and CdTe layers is performed at 500 °C. This temperature is sufficiently high, compared to the softening point of the glass, to enable the diffusion of Si and Na. In has a high concentration (between 10^{19} and 10^{22} cm⁻³, Fig. 3) compared to its concentration in the CdCl₂ powder (0.94 ppm or about 2.5×10^{16} cm⁻³) and also to its concentration in the CdTe layer measured from the back wall (3×10^{16} – 6×10^{16} cm⁻³).⁹ From these comparisons, we can deduce that In is mainly originating from the In₂O₃:F TCO used and that the contribution from CdCl₂ is negligible. As for Zn, which was not detected in the CdCl₂ powder (Table I), the concentration recorded in CdS [$(2\text{--}5) \times 10^{19}$ cm⁻³, Fig. 3] is at least one order of magnitude higher than that measured in CdTe from the back wall.⁹ This difference is most likely due to the fact that different isotopes were monitored for the CdS layer (⁶⁶Zn for this study) and the CdTe layer (⁶⁴Zn for the back wall SIMS). The above quantitative comparisons between the impurity concentrations measured in CdS from the front wall and in CdTe from the back wall are valid regardless of the difference in the diffusion coefficient that these impurity species may have in CdS versus CdTe.

Te depth profiles shown in Fig. 4(b) highlight the migration of Te from CdTe into the CdS layer following the CdCl₂ heat treatment, since the concentration of Te in CdS is slightly higher for the treated structure compared to the untreated one. Similar observations were reported by many authors, and, in particular, recently by Kim *et al.*¹⁵

The profiles of Na [Fig. 1(a)], S [Fig. 4(a)], and Si [Fig. 3(b)] for the untreated sample show a double peak in the CdS layer, which disappears becoming a single peak in the treated sample. This observation was repeated several times in different areas of the untreated sample. The most likely explanation of this behavior is that, for some reason, the ion yields at the CdS/TCO and CdTe/CdS interfaces were enhanced for these species in the untreated structure.

In studying the distribution of impurities in the CdS, particular care was taken to establish the positions of the concentration peaks for Cl, Na, and S. In a previous report,¹⁰ these elements had been reported as having peaks that were displaced with respect to one another, the cations being closer to the TCO than the anions. The displacement had been attributed to the field structure at the interfaces.¹⁰ Other authors had also reported SIMS evidence of the segregation of Sb to the CdS/TCO interface in support of an electrical measurement of impurity distribution.¹¹ In the present work, however, the peaks for Cl, Na, and S were located at a depth of 0.86 μm from the TCO free surface, this being a reproducible finding. Since the earlier work was done in the back wall SIMS geometry, a small error in the sputter rates determined for positive and negative SIMS would result in a significant registration error between the two profiles. There

could also be uncertainty about the exact location of peaks with respect to the interfaces. We conclude that there is no displacement between the positive- and negative-ion concentration peaks and that the previous work was likely to be in error.^{10,11}

V. CONCLUSIONS AND SUMMARY

Using SIMS, we quantitatively studied the concentration and distribution of impurity species in uncontacted CdTe/CdS/TCO/glass solar cell-like structures. The SIMS depth profiling proceeded from the TCO free surface through the CdS and CdTe layers, after the glass substrate was removed. Two structures were investigated, and only one of them was postgrowth CdCl₂ heat treated in order to determine the influence of the CdCl₂ heat treatment on the distribution and concentration of impurities in the structures. The focus was on the impurity species present in the CdS layer that may have an electrical activity ultimately affecting the performance of the CdTe/CdS device. Potential origins of such impurities and their concentration changes were discussed and compared to the SIMS measurements previously obtained on the same structures from the “back wall.”

The findings of the present study can be summarized as follows.

(1) Following the CdCl₂ heat treatment, Cl and Sb impurities had higher concentrations in CdS, with Na being slightly increased. For the as-grown samples, Na was concentrated at the CdTe/CdS and the CdS/TCO interfaces, while processing caused the peak concentrations to shift to the CdS layer itself.

(2) Pb, O, Sn, and Cu conserved their concentration in CdS on the CdCl₂ treatment.

(3) Zn, Si, and In showed slightly lower concentrations in CdS after the CdCl₂ heat treatment, this reduction being explained by the volatility of the chlorides of these elements.

(4) Si and Na were mainly originating from the glass substrate during the growth and/or treatment steps.

(5) In and O were mostly due to the In₂O₃:F layer used as TCO.

(6) After processing with CdCl₂ the concentration peaks of Cl, Na, and S were positioned at the same point in the CdS layer, regardless of whether they are positive or negative species. Earlier reports of an ion displacement effect^{10,11} are attributed to an error of measurement.

This study shows the advantages of using “front wall” SIMS geometry for the superior and reliable resolution it provides. It also shows the direct implication that the fabrication steps (i.e., growth and treatment) and their reproducibility may have on the concentration and distribution of impurities in the solar cell structures. The possible relationship between the impurity profiles in the structures and the device performance, its reproducibility and stability needs to be further investigated.

ACKNOWLEDGMENTS

The authors would like to thank A. J. Pidduck and A. J. Simons for SIMS measurements, and C. Jeynes and N. Peng (Ion Beam Centre, the University of Surrey) for CdS implants. They are also thankful to the EPSRC for financial support under Grant No. GR/R39283/01.

¹J. Kokaj and A. E. Rakhshani, J. Phys. D **37**, 1970 (2004).

²D. L. Batzner, A. Romeo, M. Terheggen, M. Dobeli, H. Zogg, and A. N. Tiwari, Thin Solid Films **451–452**, 536 (2004).

³J. H. Lee, J. S. Yi, K. J. Yang, J. H. Park, and R. D. Oh, Thin Solid Films **431–432**, 344 (2003).

⁴Y. Kashiwaba, K. Isojima, and K. Ohta, Sol. Energy Mater. Sol. Cells **75**, 253 (2003).

⁵A. I. Oliva, R. Castro-Rodriguez, O. Solis-Canto, V. Sosa, P. Quintana, and J. L. Pena, Appl. Surf. Sci. **205**, 56 (2003).

⁶J. Heo, H. Ahn, R. Lee, Y. Han, and D. Kim, Sol. Energy Mater. Sol. Cells **75**, 193 (2003), and references therein.

⁷R. Dhere *et al.*, *Proceedings of the 26th Photovoltaic Specialists Conference*, Anaheim, CA, 30 September–3 October 1997 (IEEE, New York, 1997), p. 435.

⁸S. E. Asher, F. S. Hasoon, T. A. Gessert, M. R. Young, P. Sheldon, J. Hiltner, and J. Sites, *Proceedings of the 28th Photovoltaic Specialists Conference*, Anchorage, AK, 15–22 September 2000 (IEEE, New York, 2000), p. 479.

⁹M. Emziane, K. Durose, N. Romeo, A. Bosio, and D. P. Halliday, Thin Solid Films **480–481**, 377 (2005).

¹⁰K. Durose, M. A. Cousins, D. S. Boyle, J. Beier, and D. Bonnet, Thin Solid Films **403–404**, 396 (2002).

¹¹D. L. Batzner, G. Agostinelli, M. Campo, A. Romeo, J. Beier, H. Zogg, and A. N. Tiwari, Thin Solid Films **431–432**, 421 (2003).

¹²M. Emziane, C. J. Ottley, K. Durose, and D. P. Halliday, J. Phys. D **37**, 2962 (2004).

¹³D. S. Boyle, S. Hearne, D. R. Johnson, and P. O’Brien, J. Mater. Chem. **9**, 2879 (1999).

¹⁴K. Nakamura, M. Gotoh, T. Fujihara, T. Toyama, and H. Okamoto, Sol. Energy Mater. Sol. Cells **75**, 185 (2003).

¹⁵S. Kim, Y. L. Soo, G. Kioseoglou, Y. H. Kao, and A. D. Compaan, J. Appl. Phys. **96**, 1007 (2004).